

**EFFECT OF CYCLIC HEAT TREATMENT ON MICROSTRUCTURE EVOLUTION OF TA15 TITANIUM ALLOY**

To investigate the effect of cyclic heat treatment on the microstructure evolution of titanium alloys, TA15 alloys were subjected to different numbers of heat treatment cycles at various temperatures in the ( $\alpha + \beta$ ) two-phase region. The resulting microstructure and hardness of the alloy were characterized by using the metallographic microscopy, scanning electron microscopy, and Vickers hardness testing. The morphology of the initial TA15 alloy was nearly equiaxed structure. The  $\alpha$  phase content, thickness of the oxygen-rich  $\alpha$  layer, and hardness of the TA15 alloy increased with the number of cycles. The morphology of the TA15 alloy changed into the Widmannstatten structure when the alloy underwent six cycles of heat treatment between 970 and 800°C. The thickness of the oxygen-rich  $\alpha$  layer and hardness of the alloy increased with the lower limit temperature of the cyclic heat treatment. Compared with the number of cycles, the lower limit temperature of the cyclic heat treatment was a more significant factor on the microstructure evolution of the TA15 titanium alloy.

*Keywords:* TA15 titanium alloy; Cyclic heat treatment; Microstructure evolution

**1. Introduction**

Titanium alloys are used in the aerospace, military, biomedical, and chemical industries because of their high toughness, strength, and corrosion resistance [1]. There are two main phases in titanium alloys, namely, the  $\alpha$  and  $\beta$  phases. The  $\alpha$  phase, which has a hexagonal closed packed (HCP) structure, is stable at room temperature and can be transformed into the  $\beta$  phase, which has a body-centered cubic (BCC) structure. Titanium alloys can be classified into  $\alpha$ ,  $\beta$ , and ( $\alpha + \beta$ ) types based on the content of  $\alpha$  and  $\beta$  phases. TA15 titanium alloy (Ti-6.5Al-2Zr-1Mo-1V) is a near- $\alpha$  titanium alloy with high aluminum content. The main strengthening mechanism of TA15 alloy is solution strengthening of the stable element Al in the  $\alpha$  phase. The stable elements Mo and V in the  $\beta$  phase and neutral element Zr are also added to improve the processing properties [2,3]. Therefore, TA15 titanium alloy has not only the high thermal strength and weldability of  $\alpha$ -type titanium alloys, but also the plasticity of ( $\alpha + \beta$ )-type titanium alloys. These good comprehensive properties have led to the widespread use of TA15 alloy in the aviation field. It is an important material for aircraft engines as well as the structural parts of aircraft and other equipment [4-6].

Common treatment processes for titanium alloys such as deformation heat treatment [7-9] and annealing treatment [10-12] usually involve multiple processes in which the cooling process from holding temperature to room temperature may take a certain amount of time. When titanium alloys undergo quenching from high temperatures during solution and aging heat treatment, large internal stresses may be introduced, which leads to changes in size [13,14]. The quenching process is usually followed by an aging treatment to precipitate the second strengthening phase and stabilize the size of the alloys [15,16]. This leads to additional factors that need to be controlled to perform the heat treatment process properly. Cyclic heat treatment can simplify the intermediate cooling step and improve the properties of titanium alloys to some extent, which greatly reduces the time and processing cost. The influence of cyclic thermal treatments on the oxidation behavior of Ti-6Al-2Sn-4Zr-2Mo alloy was investigated by Fargas et al. It is found that cyclic treatments have a more significant role in increasing the weight gain compared to isothermal treatments [17]. In addition,  $\beta$ -segregation can be eliminated at the grain boundary and interlamellar regions of Ti-46Al-6Nb titanium alloy by extending the holding time and increasing the number of heat treatment cycles [18].

<sup>1</sup> SHENYANG AEROSPACE UNIVERSITY, KEY LABORATORY OF FUNDAMENTAL SCIENCE FOR NATIONAL DEFENSE OF AERONAUTICAL DIGITAL MANUFACTURING PROCESS SHENYANG 110136, CHINA

<sup>2</sup> SHENYANG AEROSPACE UNIVERSITY, SCHOOL OF MATERIALS SCIENCE AND ENGINEERING, SHENYANG 110136, CHINA

<sup>†</sup> These authors contributed equally to this work and should be considered co-first authors

\* Corresponding author: nzsfir@163.com



Most cyclic heat treatments can eliminate the Widmannstatten structure in titanium alloys and make the spheroidization of  $\alpha$  phase occur [19-22]. Moreover, because cyclic heat treatment is a simple and low-cost process, it is greatly significant to investigate the cyclic heat treatment process. In this study, the effects of different lower limit temperatures and number of cyclic heat treatment on the microstructure, oxygen-rich layer, and hardness of TA15 titanium alloy are investigated to obtain a processing method that can not only improve the microstructure and properties of TA15 titanium alloy but also reduce its industrial cost.

## 2. Experimental methods

Test samples with the dimensions of 10 mm  $\times$  10 mm  $\times$  5 mm were extracted from hot-processed TA15 titanium bars which were produced by the Baoji Titanium Industry Company Limited. The production process of this hot-processed TA15 bar was that after an upsetting and drawing treatment at 1150°C, the as-cast TA15 ingot was processed by a forging treatment with 40% deformation at 1050°C, and finally by an annealing treatment at 800°C for 2 h. The mass fraction composition of TA15 is Al (6.70%), Mo (1.80%), V (2.20%), Zr (2.20%), Si (0.02%), Fe (0.04%), C (0.01%), N (0.01%), H (0.02%), and O (0.13%), and the remaining composition is Ti. Metallographic tests indicated that the phase transition point of the TA15 alloy was 1010°C. The initial microstructure of the TA15 alloy before cyclic heat treatment is shown in Fig. 1. It can be seen that there was a large amount of equiaxed  $\alpha$  phase and stripe-shaped  $\alpha$  phase in the TA15 alloy. Moreover, some transformed  $\beta$  morphologies were clearly observed. It is worth noting that the appearance of the stripe-shaped  $\alpha$  phase was due to the extraction of the TA15 alloy samples from hot-processed bars. It is obvious that the initial microstructure of the TA15 alloy was close to the equiaxed structure of titanium alloys.

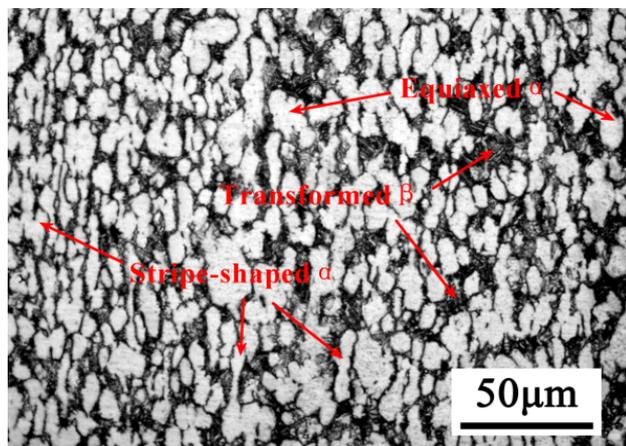


Fig. 1. Initial microstructure of the TA15 alloy

A resistance furnace was used for heat treatment in the cyclic heat treatment experiments. The cyclic heat treatment process is shown in Fig. 2. After the sample was kept in the heat

treatment furnace at the upper limit temperature for 10 min, the sample was removed and placed in the heat treatment furnace at the lower limit temperature for 10 min. The process was repeated, following which the sample was cooled by air cooling. This constitutes a complete two-cycle heat treatment process. Based on the results of the phase transition point, 970°C was set as the upper limit temperature of the cyclic heat treatment, while the lower limit temperature was set at 650°C, 700°C, 750°C, or 800°C. Two, four, six, or eight cycles were performed on the samples with a holding time of 10 min for each heating.

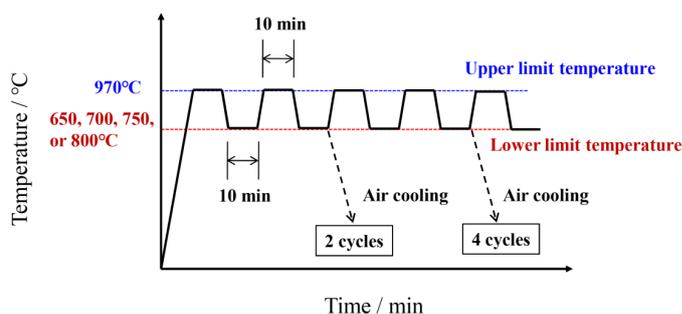


Fig. 2. Cyclic heat treatment process

Before the morphologies of the samples with different heat treatment conditions were observed by optical microscopy (OM) and scanning electron microscopy (SEM; Zeiss Sigma), the Kroll reagent with a volume percentage ratio of HF:HNO<sub>3</sub>:H<sub>2</sub>O = 2:3:95 was used to corrode the polished TA15 alloy samples for 5-10 s. Hardness measurements were performed by using a MHV-1000Z Vickers hardness tester under a load of 0.49 N for 15 s.

## 3. Results and discussions

### 3.1. Effect of cyclic heat treatment on microstructures

Fig. 3 shows the microstructure of the TA15 alloy after six cycles of cyclic heat treatment at the lower limit temperatures of 650°C, 700°C, 750°C, and 800°C. The primary  $\alpha$  phase became coarser and spheroidized, and its content increased obviously as the lower limit temperature increased to up to 700°C. Part of the  $\alpha$  phase gradually transformed from the sphere to the strip. When the lower limit temperature exceeded 750°C, the content of the equiaxed  $\alpha$  phase decreased obviously with increasing temperature. After heat treatment at 750°C, the morphology of the alloy was nearly a two-state structure, which changed into the Widmannstatten structure when the temperature increased to 800°C.

In the microstructures obtained by using optical microscopy, the white areas correspond to the  $\alpha$  phase, and the dark areas refer to the transformed  $\beta$  microstructures. The content of the  $\alpha$  phase can therefore be determined from the contrast difference of the photographs. Fig. 4 shows the curves for the  $\alpha$  phase content of the TA15 titanium alloy samples after cyclic heat treatment at different lower limit temperatures and numbers of cycles. The

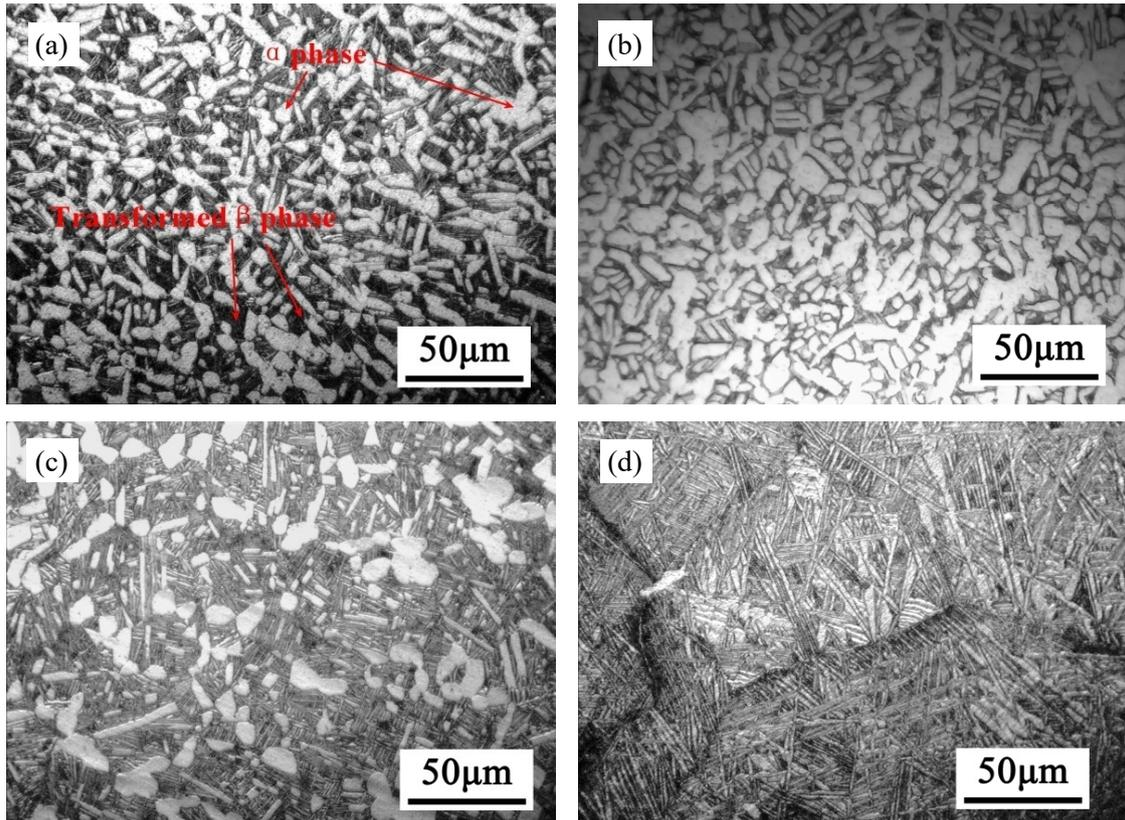


Fig. 3. Microstructures of TA15 alloy after cyclic heat treatment at the lower limit temperatures of 650°C (a), 700°C (b), 750°C (c), and 800°C (d)

sample with zero cycles corresponds to the untreated titanium alloy sample. It can be seen that for a given number of cycles, the content of the  $\alpha$  phase initially increased and then decreased with increasing lower limit temperature. The  $\alpha$  phase content was maximized at the lower limit temperature of 700°C. For a given lower limit temperature, the  $\alpha$  phase content increased with the number of cycles, but had a smaller value compared to the initial state of the TA15 alloy at the beginning of the cyclic heat treatment. This may be because the lower limit temperature

became closer to the phase transition point of the TA15 titanium alloy as the cyclic heat treatment temperature increased, which led to a reduction of the  $\alpha$  phase content. The Widmannstatten structure was formed at 800°C (Fig. 3d). Meanwhile, the  $\alpha$  phase content was the lowest at 800°C compared to the other lower limit temperatures when the number of cycles was four. This is because after four cycles of 970 ↔ 800°C heat treatment, most of the TA15 alloy microstructure changed into a finer Widmannstatten structure which could not be distinguished from the transformed  $\beta$  microstructure. However, when the number of cyclic heat treatment cycles reached six, the microstructure of the alloy completely changed into a Widmannstatten structure with a larger acicular structure compared to the structure formed after four cycles of heat treatment. This resulted in an increase of the  $\alpha$  content. Therefore, it can be concluded that the lower limit temperature should not be too high during the cyclic heat treatment of TA15 titanium alloy.

Fig. 5 shows the microstructures of TA15 alloy after two, four, six, and eight cycles of cyclic heat treatment at the lower limit temperature of 700°C. A large number of striped  $\alpha$  phases and a small amount of equiaxed  $\alpha$  phases were observed in the TA15 alloy. Meanwhile, a small amount of needled  $\alpha$  phase was also formed. As the number of cycles increased, the striped  $\alpha$  phase became coarser and gradually transformed into the equiaxed  $\alpha$  phase.

Combined with the variational trend of the  $\alpha$  phase content in Fig. 4, it can be seen that the  $\alpha$  phase content increased with the number of heat treatment cycles. This is because the  $\alpha$  phases

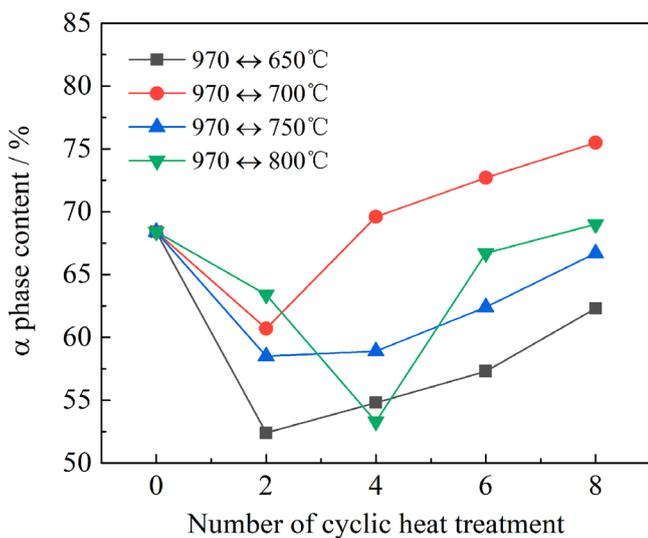


Fig. 4. Curves of the variation of the  $\alpha$  phase content with the number of cyclic heat treatment cycles for TA15 titanium alloy

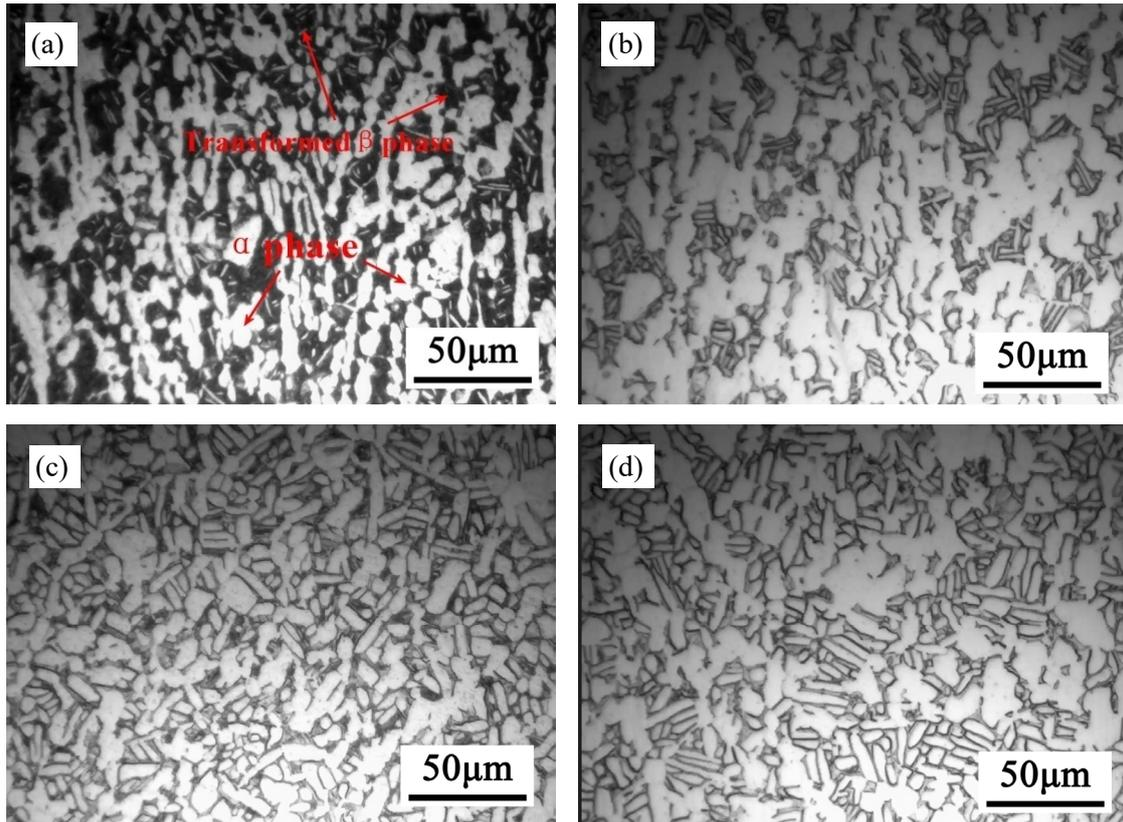


Fig. 5. Microstructures of TA15 alloy after two (a), four (b), six (c), and eight (d) cycles of cyclic heat treatment at the lower limit temperature of 700°C

would increasingly contact and combine with one another during the cyclic heat treatment in the two-phase region of low-temperature. This resulted in spherulicity and the formation of stripes in TA15 alloy as the number of cycles and, therefore, the heat treatment time, increased.

### 3.2. Effect of cyclic heat treatment on oxygen-rich $\alpha$ layer

The oxygen-rich layer on the surface of the TA15 alloy sample with six cycles of treatment at the lower limit temperature of 800°C is shown in Fig. 6. Owing to the invasion of oxygen atoms

during heat treatment, an oxygen-rich  $\alpha$  layer with high oxygen content was formed on the surface of the titanium alloy after heat treatment, as shown in the highlighted area in Fig. 6a. Because oxygen is a stable element of the  $\alpha$  phase in titanium alloys, the oxygen-rich  $\alpha$  layer was mainly composed of coarse  $\alpha$  phase. As can be seen from the SEM image in Fig. 6b, although there was a Widmannstatten structure in the alloy matrix, the coarse  $\alpha$  phase was dominant in the oxygen-rich layer, which was close to the equiaxed structure. The thickness of the oxygen-rich layer formed on the surface of the sample was measured to be 34.7  $\mu\text{m}$ .

The thickness of the oxygen-rich  $\alpha$  layers on the surface of the TA15 titanium alloy samples after cyclic heat treatment was measured and shown in Fig. 7. The sample with zero cycles

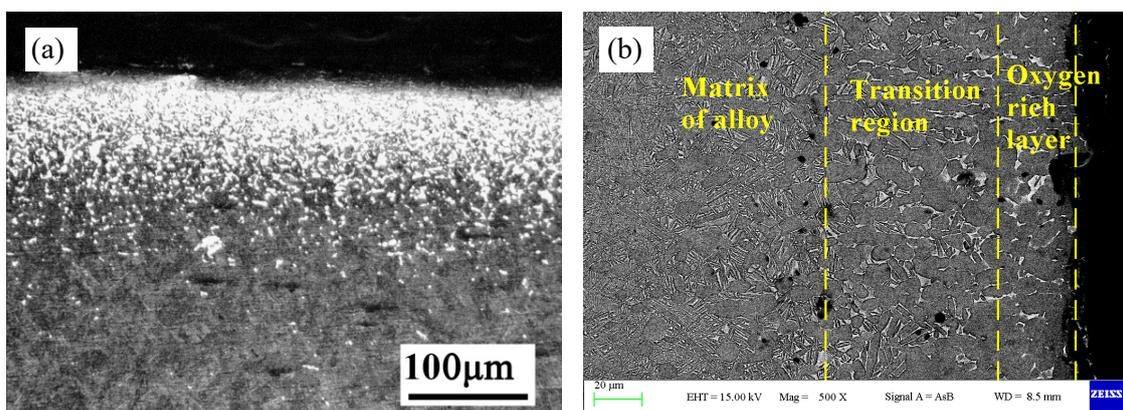


Fig. 6. OM (a) and SEM (b) images of the oxygen-rich layer in the sample treated for six cycles at the lower limit temperature of 800°C

refers to the untreated alloy. It can be seen from the curves that the thickness of the oxygen-rich  $\alpha$  layer gradually increased with the lower limit temperature and the number of cycles (i.e., heat treatment time). This increase in thickness may be attributed to oxygen diffusion. As the heat treatment time and lower limit temperature of the cyclic heat treatment increased, oxygen atoms had more energy and time to diffuse into the matrix of the TA15 titanium alloy, which resulted in the continuous thickening of the oxygen-rich  $\alpha$  layer.

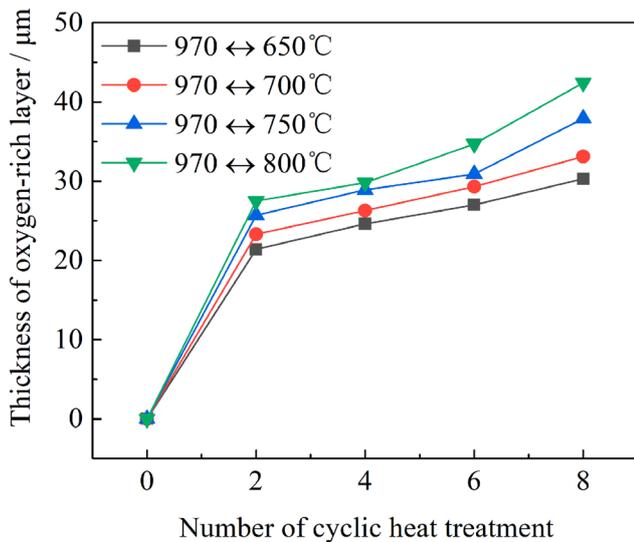


Fig. 7. Variation of oxygen-rich layer thickness in TA15 titanium alloy with the number of cyclic heat treatment

### 3.3. Effect of cyclic heat treatment on hardness

To investigate the effect of cyclic heat treatment on the hardness of TA15, the hardness of the oxygen-rich layer and the matrix alloy was measured. Fig. 8a shows the variation of the hardness from the surface to the matrix alloy after eight cycles of 970 ↔ 800°C cyclic heat treatment. It can be seen that the hardness of the TA15 alloy surface was high while that of the matrix alloy was low. This indicates that the hardness of the oxygen-rich layer was higher than that of the matrix alloy. In addition, the hardness decreased with increasing distance from the surface to the matrix, and there was an obvious transition point in the hardness curve at about 45.5  $\mu\text{m}$ . This implies that the thickness of the oxygen-rich layer measured from the hardness was 45.5  $\mu\text{m}$ , which is consistent with the optical microscopy results (Fig. 7). Fig. 8b shows the hardness curves of the TA15 alloy after different numbers of cyclic heat treatment. The sample with zero treatments corresponds to the alloy in its initial state. Because the hardness of the oxygen-rich layer varied with the distance (Fig. 8a), the hardness at approximately 15  $\mu\text{m}$  from the surface was taken as the hardness of the oxygen-rich layer to facilitate the hardness comparison of oxygen-rich layers obtained under different cyclic heat treatment conditions. This approach is reasonable because the thicknesses of all the oxygen-rich layers were larger than 20  $\mu\text{m}$  (Fig. 7) and the width of the indentation

in the hardness test was only approximately 12  $\mu\text{m}$ . It can be seen that the hardness of the oxygen-rich layer was always higher than that of the matrix alloy under different cyclic heat treatment conditions, and the Vickers hardness values were between 580 and 630. There was no obvious regularity in the hardness of the oxygen-rich layer under different processes because of the higher hardness values. The hardness of the matrix alloy in the TA15 alloy samples decreased with an increase in the lower limit temperature of the cyclic heat treatment, and showed an upward trend when the number of cyclic heat treatment cycles increased. This may be because the  $\alpha$  phase in titanium alloy has a hexagonal crystal structure with a higher hardness. As the number of cycles increased, the  $\alpha$  phase content increased, leading to a harder alloy. When the TA15 alloy was processed at 970°C /10 min ↔ 800°C /10 min, the morphology of the alloy changed greatly from the equiaxed or duplex structure to the Widmanstatten structure. The resulting alloy had a larger organizational stress, which caused its hardness value to fluctuate with the number of cycles.

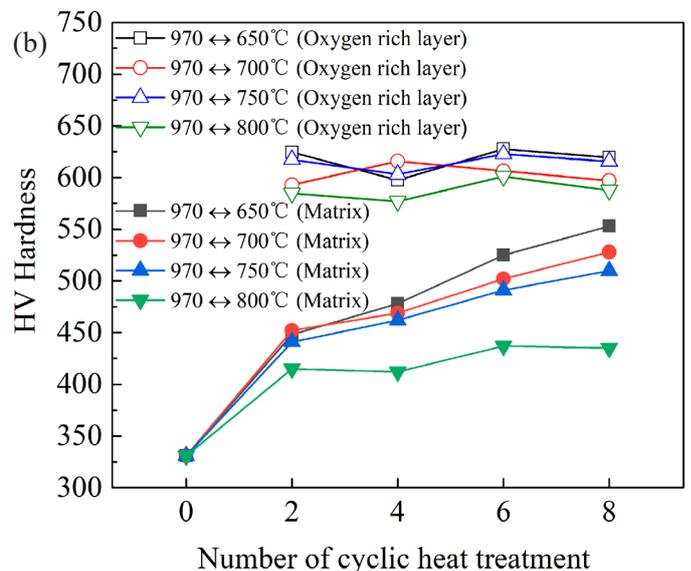
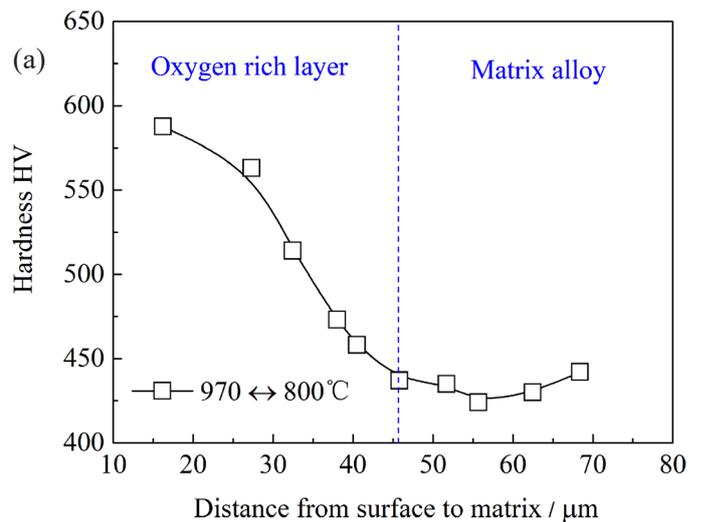


Fig. 8. Variation of hardness from surface to matrix alloy (a) and with the number of heat treatment cycles (b) for TA15 titanium alloy

#### 4. Conclusions

- (1) As the lower limit temperature of the cyclic heat treatment increased, the content of the  $\alpha$  phase in TA15 titanium alloy initially increased and then decreased. The  $\alpha$  phase content increased with the number of cycles.
- (2) When the lower limit temperature was raised to 800°C, the morphology of the alloy changed from a duplex structure to a Widmanstätten structure.
- (3) Owing to the diffusion of oxygen atoms, the thickness of the oxygen-rich  $\alpha$  layer on the surface of the TA15 alloy increased with the lower limit temperature of the cyclic heat treatment and the number of cyclic heat treatment cycles.
- (4) The hardness of the TA15 alloy can be increased by increasing the number of cycles and decreasing the lower limit temperature of the cyclic heat treatment.

#### Acknowledgments

This research was supported by the National Natural Science Foundation of China (No. 51701128), Liaoning Revitalization Talents Program (No. XLYC2007075) and the Scientific Research Fund of Liaoning Provincial Education Department (No. JYT19037).

#### REFERENCES

- [1] J. Yao, T. Suo, S. Zhang, F. Zhao, H. Wang, J. Liu, Influence of heat-treatment on the dynamic behavior of 3D laser deposited Ti-6Al-4V alloy. *Mater. Sci. Eng. A* **677**, 153-162 (2016).
- [2] X.Q. Jiang, X.G. Fan, M. Zhan, R. Wang, Y.F. Liang, Microstructure dependent strain localization during primary hot working of TA15 titanium alloy: Behavior and mechanism, *Mater. Des.* **203**, 109589 (2021).
- [3] Y. Li, P. Gao, J. Yu, S. Jin, S. Chen, M. Zhan, Mesoscale deformation mechanisms in relation with slip and grain boundary sliding in TA15 titanium alloy during tensile deformation, *J. Mater. Sci. Technol.* **98**, 72-86 (2022).
- [4] Q.J. Sun, X. Xie, Microstructure and mechanical properties of TA15 alloy after thermo-mechanical processing, *Mat. Sci. Eng. A* **724**, 493-501 (2018).
- [5] A. Arab, P. Chen, Y. Guo, Effects of microstructure on the dynamic properties of TA15 titanium alloy, *Mech. Mater.* **137**, 103121 (2019).
- [6] J. Zhao, L. Lv, G. Liu, K. Wang, Analysis of deformation inhomogeneity and slip mode of TA15 titanium alloy sheets during the hot tensile process based on crystal plasticity model, *Mat. Sci. Eng. A* **707**, 30-39 (2017).
- [7] H.Z. Guo, Z.K. Yao, L. Fang, Z.W. Su, Z.X. Wang, Y.G. Guo, M.Y. Su, Effect of Deformation Heat-treatment on Microstructure and Properties of the Alloy Ti-1023, *Rare Met. Mater. Eng.* **29** (6), 408-410 (2000).
- [8] R.N. Elshaer, M.I. Khaled, Effect of cold deformation and heat treatment on microstructure and mechanical properties of TC21 Ti alloy, *T. Nonferr. Metal. Soc.* **30**, 1290-1299 (2020).
- [9] Y. Zhao, H.Z. Guo, M.W. Fu, Y.Q. Ning, Z.K. Yao, Fabrication of bulk ultrafine grained titanium alloy via equal channel angular pressing based thermomechanical treatment, *Mater. Des.* **46**, 889-894 (2013).
- [10] K. Wang, M. Wu, Z. Yan, D. Li, R. Xin, Q. Liu, Microstructure evolution and static recrystallization during hot rolling and annealing of an equiaxed-structure TC21 titanium alloy, *J. Alloy Compd.* **752**, 14-22 (2018).
- [11] Z.B. Zhao, Q.J. Wang, J.R. Liu, R. Yang, Effect of heat treatment on the crystallographic orientation evolution in a near- $\alpha$  titanium alloy Ti60, *Acta Mater.* **131**, 305-314 (2017).
- [12] K. Mallikarjun, S. Suwas, S. Bhargava, Effect of prior  $\beta$  processing on superplasticity of ( $\alpha$ + $\beta$ ) thermo-mechanically treated Ti-632Si alloy, *J. Mater. Proc. Technol.* **134**, 35-44 (2003).
- [13] A.P. Singh, F. Yang, R. Torrens, B. Gabbitas, Solution treatment of Ti-6Al-4V alloy produced by consolidating blended powder mixture using a powder compact extrusion route, *Mat. Sci. Eng. A* **712**, 157-165 (2018).
- [14] Y.C. Lin, Y. Tang, X.Y. Zhang, C. Chen, H. Yang, K.C. Zhou, Effects of solution temperature and cooling rate on microstructure and micro-hardness of a hot compressed Ti-6Al-4V alloy, *Vacuum* **159**, 191-199 (2019).
- [15] B. Tang, Y. Chu, M. Zhang, C. Meng, J. Fan, H. Kou, J. Li, The  $\omega$  phase transformation during the low temperature aging and low rate heating process of metastable  $\beta$  titanium alloys, *Mater. Chem. Phys.* **239**, 122125 (2020).
- [16] C. Wu, M. Zhan, Microstructural evolution, mechanical properties and fracture toughness of near  $\beta$  titanium alloy during different solution plus aging heat treatments, *J. Alloy Compd.* **805**, 1144-1160 (2019).
- [17] G. Fargas, J.J. Roa, B. Sefer, R. Pederson, M.-L. Antti, A. Mateo, Influence of cyclic thermal treatments on the oxidation behavior of Ti-6Al-2Sn-4Zr-2Mo alloy, *Mater. Charact.* **145**, 218-224 (2018).
- [18] H. Fang, R. Chen, G. Anton, J. Guo, H. Ding, Y. Su, H. Fu, Effect of cyclic heat treatment on microstructures and mechanical properties of directionally solidified Ti-46Al-6Nb alloy, *Trans. Nonferrous Met. Soc. China* **25**, 1872-1880 (2015).
- [19] R. Gaddam, B. Sefer, R. Pederson, M.-L. Antti, Oxidation and alpha-case formation in Ti-6Al-2Sn-4Zr-2Mo alloy, *Mater. Charact.* **99**, 166-174 (2015).
- [20] J.H. Chen, P.M. Rogers, J.A. Little, Oxidation behavior of several chromia-forming commercial nickel-base superalloys, *Oxid. Met.* **47**, 381-410 (1997).
- [21] Y. Zhang, D.A. Shores, Study of cracking and spalling of Cr<sub>2</sub>O<sub>3</sub> scale formed on Ni-30Cr alloy, *Oxid. Met.* **40**, 529-553 (1993).
- [22] D. Poquillon, D. Monceau, Application of a simple statistical spalling model for the analysis of high-temperature, cyclic-oxidation kinetics data, *Oxid. Met.* **59**, 409-431 (2003).